HHS Public Access

Author manuscript

Biomacromolecules. Author manuscript; available in PMC 2018 October 23.

Published in final edited form as:

Biomacromolecules. 2018 April 09; 19(4): 1234–1244. doi:10.1021/acs.biomac.8b00077.

Optimizing glutaraldehyde-fixed tissue heart valves with chondroitin sulfate hydrogel for endothelialization and shield against deterioration

Mario Lopez-Moya[1,2], **Pedro Melgar-Lesmes**[1,3,*], **Kumaran Kolandaivelu**[1,4], **Jose María de la Torre Hernández**[5], **Elazer R. Edelman**[1,4], and **Mercedes Balcells**[1,2]

[1]Massachusetts Institute of Technology, Institute for Medical Engineering and Science, Cambridge, MA, US.

[2]Bioengineering Department, Institut Quimic de Sarria, Ramon Llull Univ, Barcelona, Spain.

[3]Fundació Clínic per a la Recerca Biomèdica; Department of Biomedicine, University of Barcelona, Barcelona, Spain.

[4]Cardiovascular Division, Brigham and Women's Hospital and Harvard Medical School, Boston, MA, USA.

[5]Hospital Marqués de Valdecilla, Santander, Spain.

Abstract

Porcine glutaraldehyde-fixed pericardium is widely used to replace human heart valves. Despite the stabilizing effects of glutaraldehyde fixation, the lack of endothelialization and the occurrence of immune reactions contribute to calcification and structural valve deterioration, which is particularly significant in young patients where valve longevity is crucial. This report shows an optimization system to enhance endothelialization of fixed pericardium to mimic the biological function of a native heart valve. The glutaraldehyde detoxification together with the application of a biodegradable methacrylated chondroitin sulfate hydrogel reduces aldehydes cytotoxicity, increases the migration and proliferation of endothelial cells, the recruitment of endothelial cell progenitors, and confers thrombo-resistance in fixed pericardium. The combination of glutaraldehyde detoxification and a coating with chondroitin sulfate hydrogel promotes *in situ* mechanisms of endothelialization in fixed pericardium. We offer a new solution to improve the long-life of bioprosthetic valves and explore means of making valves suitable to endothelialization.

[*]**Corresponding author** Pedro Melgar-Lesmes, PhD, Massachusetts Institute of Technology, Cambridge, Massachusetts; 77 Massachusetts Avenue, Building E25-438., Cambridge, MA 02139. USA., Phone: +1 617-715-2026, FAX: +1 617-253-2514, pedroml@mit.edu; pmelgar@dinic.cat.

Author Contributions

M.L-M., K.K and JM.D-L-T-H performed the experiments and analyzed the data. M.L- M, P.M-L., E.R.E. and M.B. designed the experiments and wrote the manuscript.

ASSOCIATED CONTENT

Supporting Information.

The Supporting Information is available free of charge on the ACS Publications website: Supplementary Figure 1 with legend, Supplementary Figure 2 with legend, Supplementary Figure 3 with legend (PDF)

Notes

The authors declare no competing financial interest.

Graphical Abstract

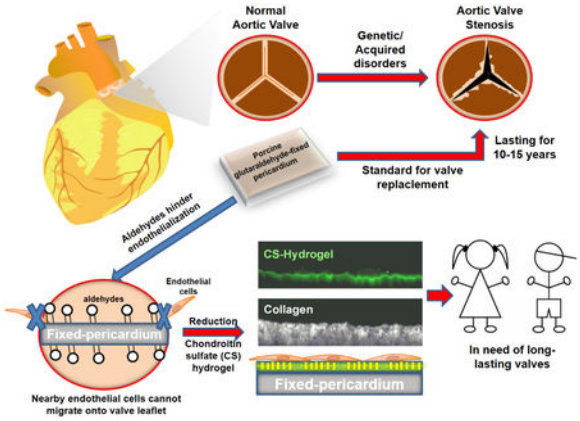

Keywords

chondroitin sulfate; hydrogel; endothelialization; aortic valve; pericardium

INTRODUCTION

Valvular heart disease is a major cause of cardiovascular morbidity and mortality with a prevalence of 2.5% in the developed countries, growing to more than 14% in patients aged 75 years and older.[1] When severe, valve replacement is the only treatment. Currently, there are an estimated 200,000 aortic valve replacements annually worldwide, a number that is expected to grow with increasing life expectancy and the introduction of transcatheter aortic valve replacement (TAVR), which stands to redefine the risk/benefit threshold of intervention.[2] The ability to perform valve-in-valve procedures reduces the morbidity of repeated procedures[3] enabling bioprosthetic implantation in younger patients while avoiding the use of mechanical valves and life-long anticoagulant therapy.

Whereas the new advances in surgical technology such as TAVR have allowed improving the efficiency and safety of implantation of valve bioprostheses, the tissue engineering to prepare the valve for implantation has been consigned to glutaraldehyde-fixed pericardium (GAP) from humans or pigs for over 50 years.[4] The main problem of using GAP are the lack of the bioactive properties of a heart valve and the appearance of a progressive process of calcification leading to structural valve deterioration and loss of function over time.[5,6] Interfering with the process of calcification is extremely relevant especially in children and young patients where valve longevity is crucial.[7] Calcification of the valve is now understood to be an active process that involves the coordinated actions of endothelial and fibroblastic cell types, circulating inflammatory and immune cells, and bone marrow-derived cells.[8-11] Repopulation and regeneration are the two main current approaches in tissue engineering to attempt to recover the bioactive properties of the heart valve.[12] A heart valve is repopulated when the patient's cells repopulate an implanted decellularized porcine aortic valve.[12] A heart valve is regenerated when an implanted resorbable matrix with patient's cells and connective tissue proteins remodels in vivo, resulting in a functional valve.[12]

However, long-term implantation studies with decellularized heart valves and acellular valves seeded with cells before implantation show tissue overgrowth, infiltration of inflammatory cells, and dilatation.[13-14] There remains the challenge to obtain valve leaflets keeping the mechanical properties of GAP but also complemented with a recovery of the versatile biological properties of the heart valve.

Endothelial cells form the luminal vascular surface and have a central role in the regulation of the haemostatic balance, coagulation, thrombosis and thrombolysis, vascular tone and growth, and in the local behavior of platelets and leucocytes.[15] The damage, the loss or the lack of this vascular endothelial layer has innumerable implications in vascular diseases.[16] In physiological conditions, healthy endothelium provides a non-permeable barrier to keep valve interstitial cells (smooth muscle cells, myofibroblasts and fibroblasts) away of circulating growth-promoting factors. Simultaneously, endothelium synthesizes growth-inhibitory factors for valve interstitial cells.[16] When endothelium is denuded or absent, such as in GAP, and implanted in substitution of a damaged heart valve, nearby smooth muscle cells might proliferate and migrate freely to the non-endothelialized valve surface. There smooth muscle cells secrete extracellular matrix proteins and attractants of platelets and leucocytes, which release growth factors and cytokines, some of them with osteogenic potential.[17] Instructed by this knowledge, we chose to optimize the surface of GAP in order to maximize the endothelialization on the basis of the following design principles: removal of all toxic aldehyde moieties in GAP, enrichment with chondroitin sulfate in a biodegradable scaffold to strongly attract endothelial cells and progenitors, to modulate macrophages, and simultaneously conferring thrombo-resistance. Herein, we engineered GAP using the above design criteria, and achieved to recapitulate the biofunctional nature of a heart valve.

MATERIALS AND METHODS

Harvesting of pig pericardium and fixation with glutaraldehide.

Five male, Yorkshire swine 12–14 weeks of age, were sedated with Telazol (10 mg/kg) and then euthanized. Animal experiments were approved by the Animal Ethics Committee at Massachusetts Institute of Technology, MA, USA. Porcine pericardium was harvested (local abattoir), washed, fixed in 0.65% glutaraldehyde for 2 weeks, and preserved in 0.2 % glutaraldehyde at 4oC. Glutaraldehyde-fixed pericardium (GAP) was selected within a range of thicknesses (250±25um) and washed three times for 5min in saline prior to use. The fixation process was followed by differential scanning calorimetry measurement of shrinkage temperature. Unfixed pericardium and commercial available pericardium were used as fixation controls.

Cell culture.

HAEC and HUVEC were cultured in EBM-2 basal medium LONZA® supplemented with 10% FBS, 1% penicillin-streptomycin, 0.04% hydrocortisone, 0.4% human fibroblast growth factor 2, 0.1% vascular endothelial growth factor, 0.1% R3-insulin-like growth factor-1, 0.1% ascorbic acid, 0.1% human endothelial growth factor, and 0.1% gentamicin-amphotericin 1000. EPC were cultured with EGM-2 supplemented with all supplements in

the bullet kit, and 20% FBS. HASMC and THP-1 cells were cultured in Dulbecco Modified Eagle Medium (DMEM) supplemented with 10% heat inactivated FBS. Cells were fed every 48h and incubated in a humidified incubator at 37°C and 5% C02. All cells were used between passages 3 to 5.

Endothelial progenitors isolation.

Blood from healthy volunteers was collected and anticoagulated with 10 U Heparin/mL. Mononuclear cells were isolated using Ficoll centrifugation for 10min at 500g. Mononuclear cells were washed with EGM-2 supplemented with 20% FBS and plated for 48h. At this point, non-adherent cells were removed. After 2 weeks culture with EGM-2 supplemented with 20% FBS, individual colonies were plated and frozen until use.

Aldehyde quantification and visualization.

ALDH-based assay: Glutaraldehyde quantification was performed using 1U/mL aldehyde dehydrogenase (Sigma-Aldrich) in 100 mM pyrophosphate buffer (pH 8.5) with oxidized nicotinamide adenine dinucleotide (0.5mM) as cofactor. The linear quantification domain was established using GAP samples of various diameters (0.78 to 6 mm). NADH quantification was carried out by measuring absorbance at 340 nm. Standard curves of NADH and GA were used for the quantification (linear 0-1mM range; n=5 per group). Lucifer yellow assay: For visual assessment, pericardial patches (n=5) were incubated with 10 μg/mL lucifer yellow for 8h. Following incubation, patches were thoroughly washed three times for 5 min with PBS before fluorescent imaging. Imaging was performed using multiphoton microscopy (Olympus FV1000MPE) in a Z-stack mode and a scanning speed of 20us/pixel and 640×640 pixels using a 20× water objective. The laser was used at an excitation wavelength of 840 nm and fluorescence recorded at 520 nm. The detector was configured to ensure saturation and linear correlation between signal intensity and tissue fluorophore content. The second harmonic generation of collagen was excited at 840 nm and detected at 420 nm.

Aldehyde elution and kinetics.

Elution kinetics of aldehydes from GAP was analyzed by incubating 2.8 cm2/mL of GAP in PBS in a continuously stirred tank under 600 rpm and orbital amplitude of 10 mm. At specified time points (0, 0.1, 0.5, 3, 24, 72h), supernatant was replaced with PBS to eliminate free aldehydes. Patches (n=5) were extracted from the tank and stored at −20°C for further analysis. Transient elution and remaining tissue-bound aldehydes were quantified using enzymatic ALDH-based assay described below.

Glutaraldehyde cytotoxicity.

The lethal concentration 50 (LC50) of HAEC, human aortic smooth muscle cells (HASMC, ATCC) and the monocyte cell line THP-1 to soluble glutaraldehyde was analyzed by seeding 104 cells/cm2 in 96 well plates (monocytes differentiated to macrophages with phorbol myristate acetate; 20 ng/mL). After 2 days, non-adherent cells were removed, and increasing concentrations of GA 0-400 μM were added to the cell culture medium (with or without

high-glucose concentration; 25mM). Cell viability was quantified after 48h using MTS (Promega®). Unfixed, viable and 1% saponin-lysed cells (10 min) served as controls.

Chemical Detoxification of GAP.

GAP was chemically detoxified by reducing aldehydes to alcohols (GAPH) via three washes of 5 min in saline followed by 12h incubation in 100 mM Sodium borohydride (Sigma-Aldrich®), and 100 mM phosphate buffer (pH=7) as previously described (23). Tissues were washed three times for 15 min in PBS with 1 % penicillin/streptomycin (Lonza®) prior to use.

Hydrogel synthesis and GAP coating.

Additional GAP and GAPH surface modification was performed through hydrogel polymerization. First, the tissues were washed 3 times for 5 min with saline solution, followed by an activation step with 0.1 M N-(3-Dimethylaminopropyl)-N'-ethylcarbodiimide hydrochloride (Sigma Aldrich®) and 0.1 M N-Hydroxysuccinimide (Sigma Aldrich®) for 15min. The tissues were then rinsed with PBS and incubated with 0.1 mg/mL of 2-aminoethyl methacrylate hydrochloride (Sigma-Aldrich®) for 2h. Tissues were then washed three times for 30 min with PBS. Chondroitin sulfate methacrylate was synthesized using 20 KDa Chondroitin sulfate (BioIberica®, Spain). Chondroitin sulfate methacrylate was polymerized using 0.5 % Irgacure 2959® as photoinitiator for 15 seconds under UV (DYMAX® Blue Wave 75) on each side of the GAP and GAPH patches. Thereafter, patches were washed three times for 15 min with PBS. When needed, fluorescence-tagged chondroitin sulfate methacrylate was synthesized by incubation with EDC/NHS 0.1 M and Fluorescein-Hydrazine at 50 μg/mL for 4h in PBS followed by purification with filters of a 3 kDa cutoff (Amicon®).

Hydrogel characterization.

GAP linked to CS hydrogel (GAPCS) and reduced GAP linked to CS hydrogel (GAPHCS) were fluorescently tagged with FITC and used to image the surface of pericardium patches after hydrogel coating. Images were obtained by multiphoton microcopy (Olympus FV1000MPE) in a Z-stack mode and a scanning speed of 20 μs/pixel and 512×512 pixels using a 20× water objective. Patches were washed extensively to detach loosely bound hydrogel. The equilibrium swelling and modulus of 1 mm thick hydrogel coating/3 mm-diameter pericardium patches (n=6) was measured using a Planar Bi-axial test system. Patches were compressed at a speed of 0.01 mm/s and compressive modulus calculated as the linear stress/strain ratio. Hydrogel biodegradability was studied by incubating 2 μL spheres of fluorescently tagged hydrogels in PBS, PBS supplemented with 10% FBS, and PBS supplemented with 10U/mL esterase from porcine liver (Sigma-Aldrich) for 23 days and quantifying soluble released fluorescence.

Albumin adsorption test.

GAP, GAPH, GAPCS and GAPHCS were incubated with 0.2 % BSA-FITC (Sigma-Aldrich) in PBS at 37°C for 2h under 600 r.p.m. in an orbital shaking (n=5 per experimental group). After three 5-min washes in PBS, multiphoton images of all patches were obtained.

Z-stack imaging was performed at sub-saturation (840 nm excitation with 520 nm detection for BSA-FITC and 420 nm detection for collagen's second harmonic generation). Tissue-adherent BSA was quantified by subtracting patch background fluorescence before and after BSA-FITC incubation.

Cell viability of HAEC seeded on GAP.

Modified and unfixed 3 mm pericardium patches were incubated in EGM-2 media supplemented with 10% FBS 1% penicillin-streptomycin for 30min prior to use. Patches (n=6) were then seeded with HAEC (25,000 cell/cm^2, passages 3-5) and cultured in EGM-2 supplemented media. Viability was tested after 48h using MTS (Promega®).

Cell proliferation assay on pericardium patches.

HAEC, HUVEC, and EPC were seeded at 10,000 cells/cm^2 on 6 mm pericardium patches (n=6). The fold increase in cell population was established by measuring cell metabolic activity using the MTS assay after 12h and 7 days. A standard MTS curve obtained with different cell numbers seeded on 96-well plates was used for the quantification.

Surface migration assay.

HAEC were seeded at a density of 30,000 cells/cm^2 over 6 mm pericardium patches (n=5) with a 3 mm PDMS insert placed in the middle. After 6h PDMS inserts were removed and patches were imaged at 6h, 2 days, and 7 days. Briefly, cells were fixed (4% paraformaldehyde) for 30min, permeabilized (0.1% Triton) for 10min, and stained with DAPI (nuclei) and TRITC-phalloidin (cytoskeleton). Cells were visualized using an Olympus FV1200 laser scanning confocal microscope. Cell migration was determined using ImageJ to quantify the amount of pericardium area cells invaded per unit of time.

Western Blot to analyze endothelial cell inflammation or health.

HAEC were seeded for 7 days over pericardium tissues and protein collected for western blotting. Cells were collected by washing twice with ice-cold PBS, and lysed with RIPA buffer supplemented with protease inhibitor cocktail. Lysates were centrifuged at 16,000g for 30 min at 4oC and supernatants were stored at −80oC until use. Protein concentration was determined using the Pierce BCA Protein Assay Kit (Pierce Biotechnology, Rockford, IL, USA). 10 μg of protein were resolved in 10% SDS-PAGE and transferred to nitrocellulose membranes. Membranes were blocked for 60 minutes in phosphate-buffered saline (PBS, Lonza) containing 0.05% Tween-20 (PBS-T, Thermo Fisher Scientific, Waltham, MA, USA) and 5% non-fat dry milk (LabScientific Inc., Livingston, NJ, USA). Then, membranes were incubated overnight in primary antibody at 4°C. Primary antibodies were diluted in PBS-T: rabbit anti-ICAM-1 (1:800, Santa Cruz), mouse anti-VCAM-1 (1:800, Thermo-Fisher), mouse anti-von Willebrand factor (1:500, Thermo-Fisher), and rabbit anti-β-actin (1:1000, Cell Signaling) as loading control. Washed membranes were incubated in horseradish peroxidase (HRP) conjugated goat anti-mouse or anti-rabbit IgG secondary antibodies (Abeam) for 45 minutes at room temperature (RT). Bands were detected directly after membrane incubation in Luminata Forte Western HRP substrate (Millipore, Bedford, MA, USA) with a chemiluminescent image analyzer ChemiDoc XRS+

System (BioRad). Blots were quantified using ImageJ software (National Institutes of Health, Bethesda, MD, USA), β-actin served as a loading control.

Thrombogenicity assay.

Blood was collected from human healthy volunteers according to the protocol approved by institutional review boards of Massachusetts Institute of Technology. Blood was immediately citrated with acid-citrate-dextrose solution (85 mM trisodium citrate, 69mM citric acid and 111 mM glucose; pH 4.6) in a 1:10 concentration and used within lh.Citrated blood was reconstituted prior to use with a solution of 100 mM CaCl2 and 75 mM MgCl2 (65 μL per milliliter of citrated blood). 200 μL of blood was added to each 3 mm-patch placed in a 96 well plate. Patches with and without endothelial cells (n=6) were rocked at 120Hz during 6 min blood incubation. The group with endothelial cells was seeded with 25,000 cells/cm^2 for 24h, washed with PBS for 1 min, and fixed with blood immediately thereafter. After incubation, blood was aspirated, and patches were washed with Tyrode's supplemented with 10 mM HEPES and 0.75 mM $MgCl_2$. After acquiring images, patches were fixed with 0.5% triton-X until clot dissolution (lh). Lysates were collected and immediately quantified by measuring the absorbance of the heme group at 405 nm. HAEC not exposed to blood and fixed with glutaraldehide (0 - 500uM) for 24h were used as negative controls.

Statistic analysis.

Data were analyzed using GraphPad Prism®. All experiments were carried out with at least sextuplicates in two independent assays. Comparisons between groups were performed by one-way ANOVA and the Tukey post-hoc test. Differences were considered significant when $p < 0.05$ *, $p < 0.01$ ** and $p < 0.001$ ***.

RESULTS

Endothelial cells are much more sensitive to aldehydes than smooth muscle cells and monocytes.

Aldehydes are mainly attached to the amine groups of collagen fibers of pericardium but they can also be just adsorbed between fibers after the fixation protocol (Figure 1A). We wondered whether both adsorbed and tissue-bound glutaraldehyde residues might hinder the tissue leaflet endothelialization as glutaraldehyde-fixed pericardium (GAP) does not endothelialize completely in vivo.[18] We then performed experiments to analyze the amount of adsorbed and tissue-bound aldehydes present in GAP quantifying the amount of released aldehydes to PBS after several washes, and the covalently-bounded aldehydes in GAP (Figure 1A). Patches obtained from GAP exponentially released aldehyde residues to the washing solvent (Phosphate-Buffered Saline, PBS) over four days after fixation of the tissue (Figure 1B). The presence of tissue aldehydes in GAP decreased over time reaching a minimum threshold of tissue-bound aldehyde moieties at around 100 nmol/cm2 after 2 days of incubation (Figure 1C). The commonly employed method to obtain fresh GAP for implantation therefore retains both free (adsorbed) and tissue-bound aldehyde residues. Fresh GAP can be washed out for days to minimize the presence of free aldehydes but tissue-bound aldehydes will remain in the tissue leaflet (Figure 1C). The inherent tissue-

bound aldehyde concentrations in washed GAP resulted more than 10 fold higher than the lethal concentration 50 (LC50) in human aorta endothelial cells (HAEC), and 4 fold higher than LC50 of human aortic smooth muscle cells (HASMC) and human THP-1 macrophages (Figure 1D). The LC50 was also tested in the absence and presence of high glucose concentration to mimic the microenvironment of patients with vascular disease caused by diabetes. Interestingly, high glucose presence negatively contributed to the survival of endothelial cells and macrophages but increased the resistance of HASMC to aldehydes (Figure 1D). The particular susceptibility of HAEC to aldehydes hampered their survival when seeded on GAP regardless of the step of the washing process and the period of aldehyde extraction (Figure 1E) These data suggest that both eluted and tissue-bound aldehydes hinder endothelialization of GAP, thus limiting its bioactive properties.

Chondroitin sulfate (CS) hydrogel and chemical reduction drastically reduce collagen-bound reactive aldehydes.

Fresh pericardium is commonly fixed with 1-glutaraldehyde, which chemically binds aldehydes to the free amine groups to the proteins of the tissue (mainly collagen) in order to obtain GAP (Figure 2A). Once we obtained GAP, we then either treated it with sodium borohydride for promoting the reduction of both free and bound aldehydes (GAPH) or cross-linked it and coated it with a CS hydrogel (GAPCS, Figure 2A). GAPH was also coated with a CS hydrogel to test synergic protective effects on GAP (GAPHCS, Figure 2A). Coating GAP with CS hydrogel significantly reduced the number of active aldehydes in GAP due to the reaction of part of them with the hydrogel compounds (Figure 2B). Chemical reduction of GAP with sodium borohydride alone or in combination with CS hydrogel completely eliminated the presence of aldehydes, thus optimizing the tissue to resemble unfixed pericardium (Figure 2B). The staining of aldehyde moieties in GAP colocalized with the fibers of tissue collagen visualized with the second harmonic of multiphoton microscopy (Figure 2C). This suggested that collagen fibers are the main reservoir of tissue-bound aldehydes in GAP as expected. The treatment of GAP with sodium borohydride alone or in combination with CS hydrogel completely abolished the staining and the presence of aldehydes in GAP (Figure 2C).

Long-lasting CS hydrogel gives surface plasticity and resistance to adsorption of blood plasma proteins.

We cross-linked the fluorophor Fluorescein-Hydrazine into the CS hydrogel to characterize the spreading and formation of the hydrogel layer onto the surface of a processed pericardium. CS hydrogel was only located on the surface of the pericardium showing a thickness of 19±4 μm attaching to the collagen layers of the tissue, which were visualized with the second harmonic signal by multiphoton microscopy (Figure 3A). As cells require specific substratum stiffness and we aim to the endothelialization of the valve leaflet, we characterized the mechanical modulus of the CS hydrogel layer. We found a modulus of 60 kPa for CS hydrogel (Figure 3B) – more than an order of magnitude softer than GAP and GAPH tissues. Therefore, CS hydrogel confers surface plasticity to the tissue as well as an enriched niche for the growth of endothelial cells. We also demonstrated the long stability of Fluorescein-linked CS hydrogel for at least 23 days performing a degradation assay with PBS, fetal bovine serum (FBS) or the hydrolase enzyme esterase (Figure 3C). After 23 days

of experiment less than 5% was degraded in all of these conditions (Figure 3C). Actually, after 10 days, degradation of CS hydrogels incubated with PBS plateaued and only progressed, and slowly, in CS hydrogels in contact with media containing FBS or esterase (Figure 3C). This resistance to degradation was highlighted by the fluorescence emitted under UV-light by the remnant CS hydrogel after 23 days (Figure 3D). To study the absorption of albumin as the most abundant blood plasma protein in contact with heart valve implants, we incubated all the different treatments of GAP with fluorescein-labeled bovine serum albumin (BSA). The presence of CS hydrogel significantly reduces the BSA adsorption in GAP (Figure 3E). However, the chemical reduction of GAP increases the adsorption of BSA in the presence or absence of hydrogel (Figure 3E), and this binding collocalized with the collagen fibers (Figure 3F). This effect can be explained by the different electrostatic interactions of BSA and the tissue-bound aldehydes in GAP or GAPH. While GAP has non-protonated imine at physiologic pH, the reduced form GAPH has protonated secondary amines that attract the negatively charged BSA (Figure 3G). This suggests that reduced GAP will show a high interaction with negatively charged proteins and low binding of positively charged blood plasma proteins.

CS hydrogel and the chemical reduction of GAP protect human endothelial cells' grown on pericardium.

We analyzed the biofunctional properties of our engineered pericardium designed to allow the survival and the growth of endothelial cells for endothelialization. Tissue- bound aldehydes did not allow growing the human endothelial cells HAEC seeded on GAP even when CS hydrogel was added to protect and enrich the surface of the tissue (Figure 4A). In contrast, the chemical reduction of GAP with or without CS hydrogel drastically prevented this inhibitory effect of aldehydes on HAEC growth, allowing a stable endothelial cell layer for 3 days (Figure 4A). Afterwards, we tested the viability of different endothelial cell types seeded on GAP and we found that the chemical reduction produced an identical protective effect in human umbilical vein endothelial cells (Figure S1A). CS hydrogel significantly protected endothelial progenitor cells (EPC) seeded on GAP, but only the reduction of GAP prevented the deleterious effects of aldehydes in EPC growth (Figure S1B). Thereafter we analyzed the impact of tissue-bound aldehydes or the treatments of pericardium on the synthesis of actin filaments. Actin is a crucial protein for endothelial cell shape change and cytoskeletal remodeling in response to fluid shear stress.[19] Endothelial cells growing on an implanted heart valve should ideally display high levels of stress fibers such as actin to correctly align and adapt to the high shear stress of blood stream in the heart. This is important because it influences the mechanic properties of the valve and also the bioactive functions and health of the tissue. Our outcomes show that although CS hydrogel preserves some of the expression of actin filaments in endothelial cells in GAP, only the chemical reduction in the presence or absence of CS hydrogel safeguards the physiological synthesis of actin for a correct morphological phenotype of endothelial cells (**Figure 4B and Figure S2**). We wondered whether tissue-bound aldehydes were triggering not only proliferation arrest and actin down-regulation but also apoptosis in endothelial cells seeded on GAP. We found that normalized activity of caspase 3/7 was 6-fold higher in endothelial cells seeded on GAP in comparison to endothelial cells seeded on GAP with CS hydrogel, or reduced pericardium with or without hydrogel (Figure 4C). The suitability of using both CS hydrogel

and the chemical reduction to eradicate the pro-apoptotic effects of GAP in endothelial cells was further demonstrated and highlighted when visualizing the binding of Annexin-V to the cell membrane marker of apoptosis phosphatidylserine. We observed both apoptosis (Annexin-V positive) and necrosis (propidium iodide positive) in GAP but no apoptosis or necrosis in GAP treated with chemical reduction and coated with CS hydrogel (Figure 4D).

CS hydrogel and the chemical reduction of GAP boost endothelialization.

We performed a migration assay of HAEC towards porcine GAP patches to analyze the possible endothelial cell migration occurring after implantation of the heart valve (for example, from the aortic root to the valve leaflets). Migration of HAEC was hindered for 7 days either in GAP or GAP coated with CS hydrogel likely due to cell death or detachment (Figure 5A). HAEC avidly migrated to the surface of the reduced pericardium with or without CS hydrogel and formed a confluent monolayer over the entire patch in less than 3 days, which remained stable for at least 7 days (Figure 5A). These migrating HAEC showed the characteristic features of a correct synthesis and assembling of cytoskeletal actin for adaptation to shear stress in contrast to HAEC in contact with non-reduced GAP (Figure 5B). Once endothelial cells migrate to the patch it is important that they proliferate to cover the surface of the implant in order to form a stable and healthy endothelium that may guard homeostasis of the tissue. Our results show that after the migration of HAEC to patches of reduced GAP, the cell population increases 2 times for 7 days, and this proliferation rate is further enhanced with the addition of CS hydrogel (Figure 5C). HAEC cultured for 7 days on the surface of aldehyde-free pericardium did not show up-regulation of the inflammatory cell surface markers ICAM-1 (Figure S3A), VCAM-1 (Figure S3B), or alterations in the synthesis of von Willebrand factor (Figure S3C) suggesting that reduced GAP with or without CS hydrogel does not induce an inflammatory phenotype on endothelial cells. Cell death precluded the possibility to quantify the inflammatory state of cells seeded on GAP and GAPCS. Then we used human umbilical vein endothelial cells as a different source of endothelial cells and we observed that both chemical reduction and CS hydrogel augmented the cell proliferation (Figure 5D). It is known that EPC recruitment and proliferation also play a role in *in situ* endothelialization after vascular or tissue injury.[20] We found that GAP with or without CS hydrogel completely blocked EPC proliferation, and even reduced the number of cells on the tissue resulting in a negative fold change of proliferation after 7 days (Figure 5E). The chemical reduction of GAP alone had no relevant effects on proliferation of EPC but, when combined with the enriched extracellular matrix environment of CS hydrogel, the combination resulted in a significant increase in EPC proliferation (Figure 5E).

CS hydrogel and the chemical reduction of GAP reduce blood clotting.

We studied the propensity of fixed tissues to induce blood clotting in the absence or the presence of HAEC to mimic both possible situations right after the implantation of the heart valve. Either CS hydrogel implanted in GAP was the most effective reducing blood clotting in acellular patches of GAP (Figure 6A). The chemical reduction of GAP with or without hydrogel also reduced significantly the blood clotting in acellular tissue leaflets as compared with GAP alone (Figure 6A). When HAEC were seeded on the tissue leaflets, CS hydrogel did not prevent the clot formation and only the chemically reduced tissue in presence or

absence of CS hydrogel diminished the clotting effects observed in GAP (Figure 6B). All of these effects on blood clotting are visualized in Figure 6C.

DISCUSSION

Novel therapeutic interventions to halt heart valve deterioration need to be focused on strategies that target the cellular events that control the degeneration and rejection of the tissue. The common problem of implanting GAP is the calcification of the valve over time leading to structural valve deterioration.[5,6] Although many efforts during decades have been focused to neutralize GAP aldehydes to stop calcification,[21-24] there has been no success to restore the long- lasting natural biological resistance to calcification of a heart valve using GAP. Herein we describe that not only covalently tissue-bound aldehydes can be found in GAP but also adsorbed aldehydes, both contributing to especially reduce the viability of endothelial cells. We show that macrophages and smooth muscle cells are four times more resistant to aldehydes than endothelial cells. This suggests that macrophages and smooth muscle cells are better qualified than endothelial cells to attach and proliferate in the implanted GAP or its environment. It has reasonably been postulated that the biological rationale for failure of glutaraldehyde-fixed tissue heart valves is an immune response to the xenograft tissue, a chronic process of inflammation, fibrosis and subsequent calcification of the valves leaded by macrophages and assisted by smooth muscle cells.[9-10,25] It is there where the design of new methods and biomaterials for long-lasting heart valves should take into account not only promoting the repair of the protective physiological barrier of endothelium but also modulating macrophages to reduce local inflammation and inhibiting the migration and proliferation of smooth muscle cells to the valve. In this context, based on its biological activity, we chose the extracellular matrix component CS to synthesize a hydrogel and attach it to GAP. CS is a glycosaminoglycan synthesized by vascular pericytes as scaffold for adhesion and migration of vascular endothelial cells and EPC.[26] CS has traditionally been associated to the prevention of cardiac events[27-28] and now we also know that CS interferes with the pro-inflammatory effects of tumor necrosis factor alpha (TNF-α) on macrophages and endothelial cells.[29] Herein we demonstrate that CS hydrogel enriches a chemically reduced GAP to display all the biofunctional properties required to behave as a physiological heart valve. CS hydrogel chemically-linked to reduced GAP is an important improvement of the traditional method of GAP reduction[21] or the use of other extracellular matrix components in hydrogel.[30] The biocompatible CS hydrogel that we designed has a very slow degradation rate to give time and scaffold support for endothelial cell migration from the aortic root when implanted. We also focused on a specific thickness of 20 μm to mimic the width of a healthy endothelium. We show that CS hydrogel has the ideal characteristics for the recruitment of nearby endothelial cells and also circulating EPCs in order to obtain an endothelial cell layer. Indeed we observed that CS hydrogel boosts the proliferation of aortic endothelial cells and EPC in GAP while shielding these cells from apoptosis. Interestingly, endothelial cells from the fetal phase corresponding to umbilical cord proliferate much faster than adult aortic endothelial cells or EPCs seeded on reduced GAP. This indicates that endothelialization of detoxified GAP is expected to be quicker in young patients and children.

Evidence indicates that valvular endothelial cells exposed to abnormal hemodynamic forces (such as hypertension, elevated stretch, or shear stresses) are partially responsible of the valve tissue remodeling and recruitment of inflammatory leukocytes, which lead to calcification, stenosis, and ultimate valve failure.[31] We show that coating with CS hydrogel reduces GAP surface modulus thus giving some mechanical plasticity to the valve leaflet. The combination of CS hydrogel with the chemical reduction also prevents the synthesis of the leukocyte adhesion molecules VCAM-1 and ICAM-1 in endothelial cells. A combination of endothelial damage and lipid deposition triggers inflammation within the valve. The expression of adhesion molecules allows infiltration of the endothelial layer by monocytes that differentiate into macrophages and T cells that release proinflammatory cytokines, including transforming growth factor-β-1, tumor necrosis factor-α, and interleukin-1-β.[32] These inflammatory cells and cytokines ultimately help stimulate and establish the subsequent fibrotic and calcific processes that drive increasing valve stiffness. The mechanical and biological shield of endothelial cells against shear stress and monocyte recruitment together with the direct activity of CS reducing monocyte and macrophage migration[29] point to CS hydrogel as an excellent biomaterial to protect bioprosthetic valves from calcification. Actually either CS or healthy endothelial cells also inhibit the migration and proliferation of fibroblastic cell types thus protecting the valve from hyperplasia.[33] Osteogenic morphogens secreted mainly by macrophages stimulate fibroblastic cell types to undergo a phenotype transition to become osteoblast-like cells and elaborate bone matrix that serve as a nidus for microcalcifications.[34] As our results show that GAPHCS prevent the synthesis of monocyte adhesion molecules in seeded endothelial cells, altogether this suggests that the combined strategy of endothelialization of GAP with CS hydrogel and chemical reduction presented here might protect the valve not only against calcification but also against fibrosis in multiple ways.

Bioprosthetic heart valve replacements reduce thromboembolic risk compared to mechanical valves, with events persisting in 1-2%.[35-36] We found that the addition of CS hydrogel coating alone or in combination with the chemical reduction provides thrombo- resistance in acellular GAP. Once host endothelialization begins, the best option to prevent clot formation is the combination of chemical reduction and CS hydrogel providing long-term antithrombotic benefits. Therefore the combination of CS hydrogel and chemical reduction protects the heart valve implant from blood clotting before and after endothelialization for long-term biosafety of the valve leaflet.

CONCLUSIONS

Most of the methods employed to endothelialize GAP for the past two decades have not been able to support endothelialization without including exogenous cell lines to make the implants viable[37-38] or dehydration and plasma deposition of a special substratum such as titanium.[39] Here we propose to mimic and use the inherent biological systems that drive healing and endothelialization in blood vessels for assisting in the incorporation of the implant in a physiological environment where the host endothelial cells can repopulate the implanted tissue and reconstitute a healthy endothelium. We use the extracellular matrix component of pericytes - CS- in a hydrogel as scaffold for attracting endothelial cells, which will synthesize antithrombotic and antifibrotic factors such as heparan sulfate[40] and will

serve as a shield against inflammatory cell recruitment, calcification and valve deterioration. This new modification of the fixed pericardium typically used for heart valve replacement could provide a great clinical benefit to patients with valve disease, especially children who require long-lasting heart valves and younger patients who cannot tolerate the risks and side effects of mechanic prosthetics such as lifelong anticoagulation therapy, high bleeding risks, and lifestyle modifications.

Supplementary Material

Refer to Web version on PubMed Central for supplementary material.

ACKNOWLEDGMENTS

We acknowledge support provided by the David H. Koch Institute for Integrative Cancer Research at the Massachusetts Institute of Technology for providing access to multiphoton microscopy used for this study.

Funding Sources

M.B. was supported in part by Fundació Empreses IQS, and a grant from Spanish Ministry of Economy, SAF2013-43302-R. E.R.E. was supported in part by grants (R01 GM 49039) from the National Institutes of Health. K.K. was supported in part by an American Heart Association Fellow to Faculty Transition Award (12FTF12080241). P.M-L. was supported by the Pla estratègic de recerca i innovació en salut (PERIS SLT002/16/00341) and then by the Beatriu de Pinos Program 2016 (BP-00236).

ABBREVIATIONS

Abbreviations and acronyms:

BSA	bovine serum albumin
EPC	endothelial progenitor cell
EST	esterase
FBS	fetal bovine serum
FP	fresh pericardium (unfixed)
GAG	glycosaminoglycan
GAP	glutaraldehyde-fixed pericardium
GAPCS	glutaraldehyde-fixed pericardium coated with hydrogel
GAPH	glutaraldehyde-fixed pericardium reduced
GAPHCS	glutaraldehyde-fixed pericardium reduced and coated with hydrogel
HAEC	human aortic endothelial cell
HUVEC	human umbilical vein endothelial cell
PBS	Phosphate-Buffered Saline
TAVR	trans aortic valve replacement

tcwp	tissue culture well plate

REFERENCES

(1). lung B; Vahanian A Epidemiology of valvular heart disease in the adult. Nat Rev Cardiol. 2011, 8, 162. [PubMed: 21263455]

(2). Lindman B; Alexander K; O'Gara P; Afilalo J Benefit, and Transcatheter Aortic Valve Replacement. Jacc Cardiovasc Interventions 2014, 7, 707–716.

(3). Eggebrecht EL; Schäfer El.; Treede EL; Boekstegers P; Babin-Ebell J; Ferrari M; Möllmann EL; Baumgartner EL; Carrel T; Kahlert P; Lange P; Walther T; Erbel R; Mehta R; Thielmann M. Valve-in-Valve Transcatheter Aortic Valve Implantation for Degenerated Bioprosthetic Heart Valves. Jacc Cardiovasc Interventions 2011, 4, 1218–1227.

(4). Carpentier A; Lemaigre G; Robert L; Carpentier S; Dubost C Biological factors affecting long-term results of valvular heterografts, J Thorac Cardiovasc Surg 1969, 58, 467–483. [PubMed: 5344189]

(5). Schoen FJ; Levy RJ Calcification of tissue heart valve substitutes: progress toward understanding and prevention. Ann Thorac Surg 2005,79,1072–1080. [PubMed: 15734452]

(6). Siddiqui RF; Abraham JR; Butany J Bioprosthetic heart valves: modes of failure. Histopathology 2009, 55, 135–144. [PubMed: 19694820]

(7). Jaquiss R Bioprosthetic Aortic Valve Replacement in the Young: A Cautionary Tale. Circulation 2014, 130, 7–9. [PubMed: 24982114]

(8). Bayrak A; Tyralla M; Ladhoff J; Schleicher M; Stock UA; Volk HD; Seifert M Human immune responses to porcine xenogeneic matrices and their extracellular matrix constituents in vitro. Biomaterials 2010, 31(14), 3793–3803. [PubMed: 20171732]

(9). Manji RA; Menkis AH; Ekser B; Cooper DKC Porcine bioprosthetic heart valves: the next generation. Am Heart J 2012, 164(2), 177–185. [PubMed: 22877802]

(10). Manji RA; Zhu LF; Nijjar NK; Rayner DC; Korbutt GS; Churchill TA; Rajotte RV; Koshal A; Ross DB Glutaraldehyde-fixed Bioprosthetic heart valve conduits calcify and fall from xenograft rejection. Circulation 2006, 114, 318–327. [PubMed: 16831988]

(11). Rattazzi M; Pauletto P Valvular endothelial cells: guardians or destroyers of aortic valve integrity? Atherosclerosis 2015, 242(2), 396–398. [PubMed: 26277631]

(12). Vesely I Heart valve tissue engineering. Circ Res 2005, 97(8), 743–755. [PubMed: 16224074]

(13). Hilbert SL; Yanagida R; Souza J; Wolfinbarger L; Jones AL; Krueger P; Stearns G; Bert A; Hopkins RA Prototype anionic detergent technique used to decellularize allograft valve conduits evaluated in the right ventricular outflow tract in sheep. The Journal of Heart Valve Disease 2004, 13(5), 831–840. [PubMed: 15473487]

(14). Opitz F; Schenke-Layland K; Cohnert TU; Starcher B; Halbhuber KJ; Martin DP; Stock UA Tissue engineering of aortic tissue: dire consequence of suboptimal elastic fiber synthesis in vivo. Cardiovasc Res 2004, 63(4), 719–730. [PubMed: 15306228]

(15). Rafii S; Butler JM; Ding BS Angiocrine functions of organ-specific endothelial cells. Nature 2016, 529(7586), 316–325. [PubMed: 26791722]

(16). Kipshidze N; Dangas G; Tsapenko M; Moses J; Leon MB; Kutryk M; Serruys P Role of the endothelium in modulating neointimal formation: vasculoprotective approaches to attenuate restenosis after percutaneous coronary interventions. J Am Coll Cardiol 2004, 44(4), 733–739. [PubMed: 15312851]

(17). Bostrom KI; Rajamannan NM; Towler DA The regulation of valvular and vascular sclerosis by osteogenic morphogens. Circ Res 2011, 109, 564–577. [PubMed: 21852555]

(18). Ishihara T; Ferrans VJ; Jones M; Boyce SW; Roberts WC Occurrence and significance of endothelial cells in implanted porcine bioprosthetic valves. Am J Cardiol 1981, 48, 443–454. [PubMed: 7270450]

(19). Malek AM; Izumo S Mechanism of endothelial cell shape change and cytoskeletal remodeling in response to fluid shear stress. J Cell Sci 1996, 109, 713–726. [PubMed: 8718663]

(20). Melgar-Lesmes P; Balcells M; Edelman ER Implantation of healthy matrix-embedded endothelial cells rescues dysfunctional endothelium and ischaemic tissue in liver engraftment. Gut 2017,66(7), 1297–1305. [PubMed: 26851165]

(21). Chen W; Schoen FJ; Levy RJ Mechanism of efficacy of 2-amino oleic acid for inhibition of calcification of glutaraldehyde-pretreated porcine bioprosthetic heart valves. Circulation 1994, 90, 323–329. [PubMed: 8026014]

(22). Vyavahare N; Hirsch D; Lerner E; Baskin JZ; Schoen FJ; Bianco R; Kruth HS; Zand R; Levy RJ Prevention of Bioprosthetic Heart Valve Calcification by Ethanol Preincubation: Efficacy and Mechanisms. Circulation 1997, 95, 479–488. [PubMed: 9008467]

(23). Connolly JM; Alferiev I; Kronsteiner LZ; Levy RJ Ethanol inhibition of porcine bioprosthetic heart valve cuspcalcification is enhanced by reduction with sodium borohydride. J Heart Valve Dis 2004, 13, 487–493. [PubMed: 15222297]

(24). Kim KC; Kim SH; Kim YJ Detoxification of glutaraldehyde treated porcine pericardium using L-arginine and NaBH4. J Thorac. Cardiovasc Surg 2011, 44(2), 99–107.

(25). Shetty R; Pibarot P; Audet A; Janvier R; Dagenais F; Perron J; Couture C; Voisine P; Després JP; Mathieu P Lipid-mediated inflammation and degeneration of bioprosthetic heart valves. Eur J Clin Invest 2009, 39(6), 471–480. [PubMed: 19490057]

(26). Thalla PK; Fadlallah H; Liberelle B; Lequoy P; De Crescenzo G; Merhi Y; Lerouge S Chondroitin sulfate coatings display low platelet but high endothelial cell adhesive properties favorable for vascular implants. Biomacromolecules 2014, 15(7), 2512–2520. [PubMed: 24927450]

(27). Morrison LM Response of ischemic heart disease to chondroitin sulfate-A, J Am Geriatr Soc 1969,17(10), 913–923. [PubMed: 4186499]

(28). Morrison LM; Enrick N Coronary heart disease: reduction of death rate by chondroitin sulfate A, Angiology ;1973, 24, 269–287. [PubMed: 4267673]

(29). Melgar-Lesmes P; Garcia-Polite F; Del-Rey-Puech P; Rosas E; Dreyfuss J; Montell E; Vergés J; Edelman ER.; Balcells M. Treatment with chondroitin sulfate to modulate inflammation and atherogenesis in obesity. Atherosclerosis 2016, 245, 82–87. [PubMed: 26714044]

(30). Camci-Unal G; Aubin H; Ahari AF; Bae H; Nichol JW; Khademhosseini A Surface modified hyaluronic acid hydrogel to capture endothelial progenitor cells. Soft Matter 2010, 6, 5120–5126. [PubMed: 22368689]

(31). Rajamannan NM; Evans FJ; Aikawa E; Grande-Allen KJ; Demer LL; Heistad DD; Simmons CA; Masters KS; Mathieu P; O'Brien KD; Schoen FJ; Towler DA; Yoganathan AP; Otto CM Calcific aortic valve disease: not simply a degenerative process: A review and agenda for research from the National Heart and Lung and Blood Institute Aortic Stenosis Working Group. Executive summary: Calcific aortic valve disease-2011 update. Circulation 2011, 124(16), 1783–1791. [PubMed: 22007101]

(32). Dweck MR; Boon NA; Newby DE Calcific aortic stenosis: a disease of the valve and the myocardium. J Am Coll Cardiol 2012; 60(19), 1854–1863. [PubMed: 23062541]

(33). Nugent HM; Rogers C; Edelman ER Endothelial implants inhibit intimal hyperplasia after porcine angioplasty. Circ Res 1999, 84(4), 384–391. [PubMed: 10066672]

(34). Leopold JA Cellular mechanisms of aortic valve calcification. Circ Cardiovasc Interv 2011, 5(4), 605–614.

(35). Mérie C; Køber L; Olsen P; Andersson C; Gislason G; Jensen J; Torp-Pedersen C Association of Warfarin Therapy Duration After Bioprosthetic Aortic Valve Replacement With Risk of Mortality, Thromboembolic Complications, and Bleeding. JAMA 2012, 308, 2118–2125. [PubMed: 23188028]

(36). Pislaru S; Hussain I; Pellikka P; Maleszewski J; Hanna R; Schaff H; Connolly H Misconceptions, diagnostic challenges and treatment opportunities in bioprosthetic valve thrombosis: lessons from a case series. Eur J Cardio-thorac 2015, 47, 725–732.

(37). Gulbins H; Pritisanac A; Pieper K; Goldemund A; Meiser B; Reichart B; Daebritz S Successful Endothelialization of Porcine Glutaraldehyde-Fixed Aortic Valves in a Heterotopic Sheep Model. Ann Thorac Surg 2006, 81, 1472–1479. [PubMed: 16564295]

(38). Gulbins H; Goldemund A; Anderson I; Haas U; Uhlig A; Meiser B; Reichart B *J* Preseeding with autologous fibroblasts improves endothelialization of glutaraldehyde-fixed porcine aortic valves. Thorac Cardiovasc Surg 2003, 125, 592–601.

(39). Guldner NW; Jasmund I; Zimmermann H; Heinlein M; Girndt B; Meier V; Flüss F; Rohde D; Gebert A; Sievers HH Detoxification and Endothelialization of Glutaraldehyde- Fixed Bovine Pericardium With Titanium Coating: A New Technology for Cardiovascular Tissue Engineering. Circulation 2009, 119, 1653–1660. [PubMed: 19289635]

(40). Kolandaivelu K; Swaminathan R; Gibson W; Kolachalama V; Nguyen-Ehrenreich K-L; Giddings V; Coleman L; Wong G; Edelman ER Stent Thrombogenicity Early in High-Risk Interventional Settings Is Driven by Stent Design and Deployment and Protected by Polymer- Drug Coatings. Circulation 2011, 123, 1400–1409. [PubMed: 21422389]

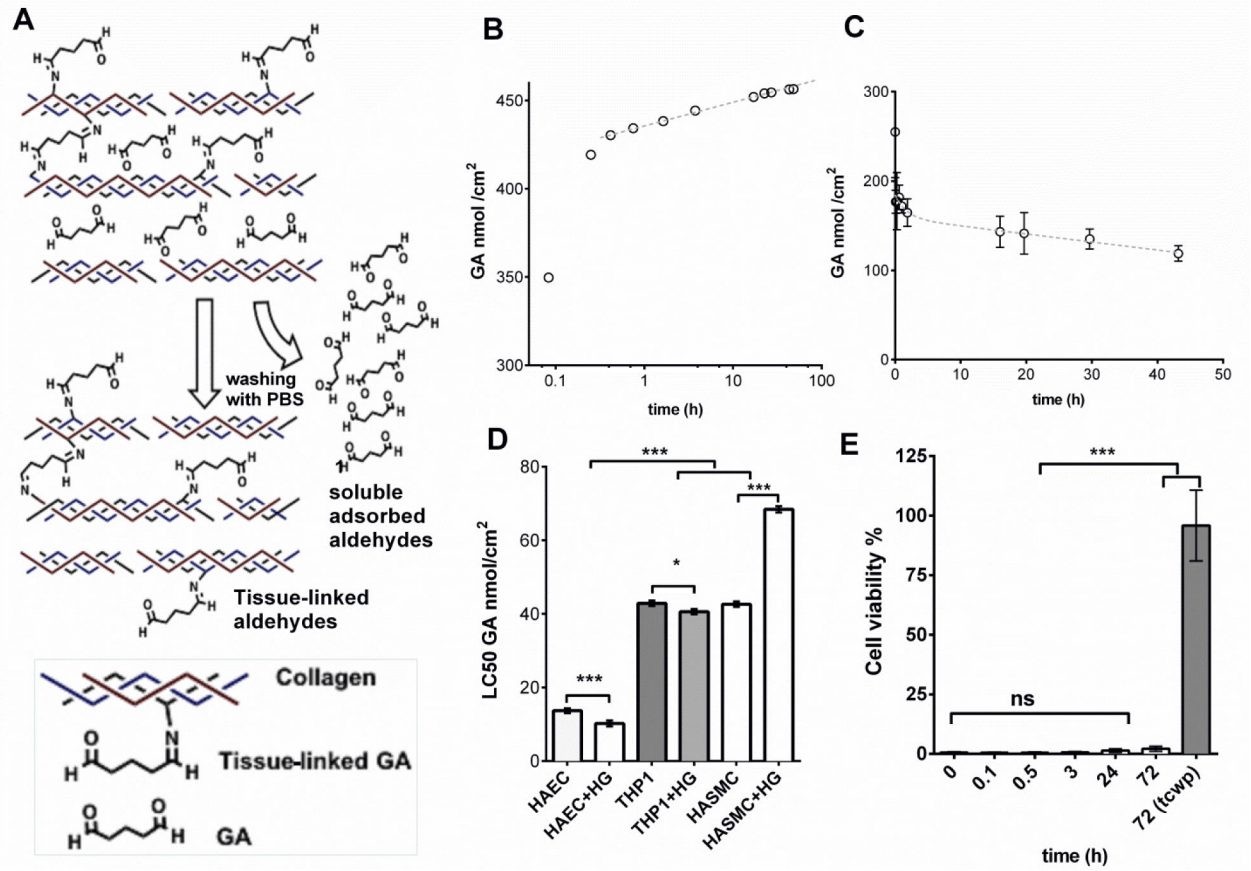

Figure 1. The presence of glutaraldehyde residues in pericardium affects the viability of endothelial cells more than vascular smooth muscle cells and monocytes.

A, Repeated washing with PBS of pericardium patches fixed with glutaraldehyde (GA) allows the elution of soluble adsorbed aldehydes, but tissue-linked aldehydes remain active and attached to the tissue collagen, **B**. Quantification of aldehydes solubilized in PBS after every washing period. **C**. Quantification of aldehydes in solid phase (tissue-linked GA) after different periods of washing. **D**, LC50 of GA in human aortic endothelial cells (HAEC), in leukemia-immortalized monocytes (THP-1) and human aortic smooth muscle cells (HASMC). The experiment was repeated with and without High Glucose (HG) at a concentration of 25 mM. **E**, Cytotoxicity assay in HAEC seeded on glutaraldehide-fixed pericardium after different periods of washing; cells grown on tissue culture well-plates (tcwp) were used as positive controls of viability (n=5). Histograms are plotted as mean ± SEM. Significant differences between the groups: * $p < 0.05$, *** $p < 0.001$.

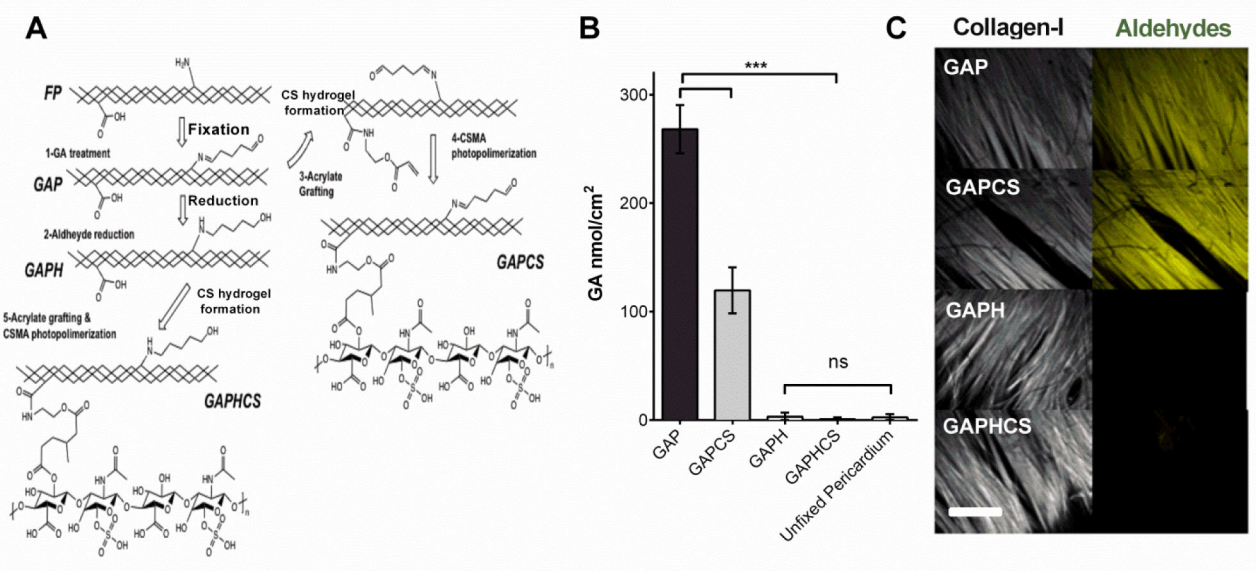

Figure 2. Design of chondroitin sulfate (CS) hydrogel and chemical reduction to eliminate collagen-bound reactive aldehydes.

A, Schematic representation of the chemical modifications in fresh unfixed pericardium (FP) in order to obtain glutaraldehyde-fixed pericardium (GAP). Once fixed, GAP was either directly coated with chondroitin sulfate hydrogel (GAPCS) or chemically reduced (GAPH) and then cross-linked with chondroitin sulfate to form a hydrogel (GAPHCS). **B,** Enzymatic quantification of the aldehydes linked to the tissue (n=5). **C,** Imaging of collagen fiber by the second harmonic generation of multiphoton microscopy (white) and staining of aldehyde moieties using Lucifer yellow (yellow). Histograms are plotted as mean ± SEM. Significant differences between the groups: *** $p < 0.001$.

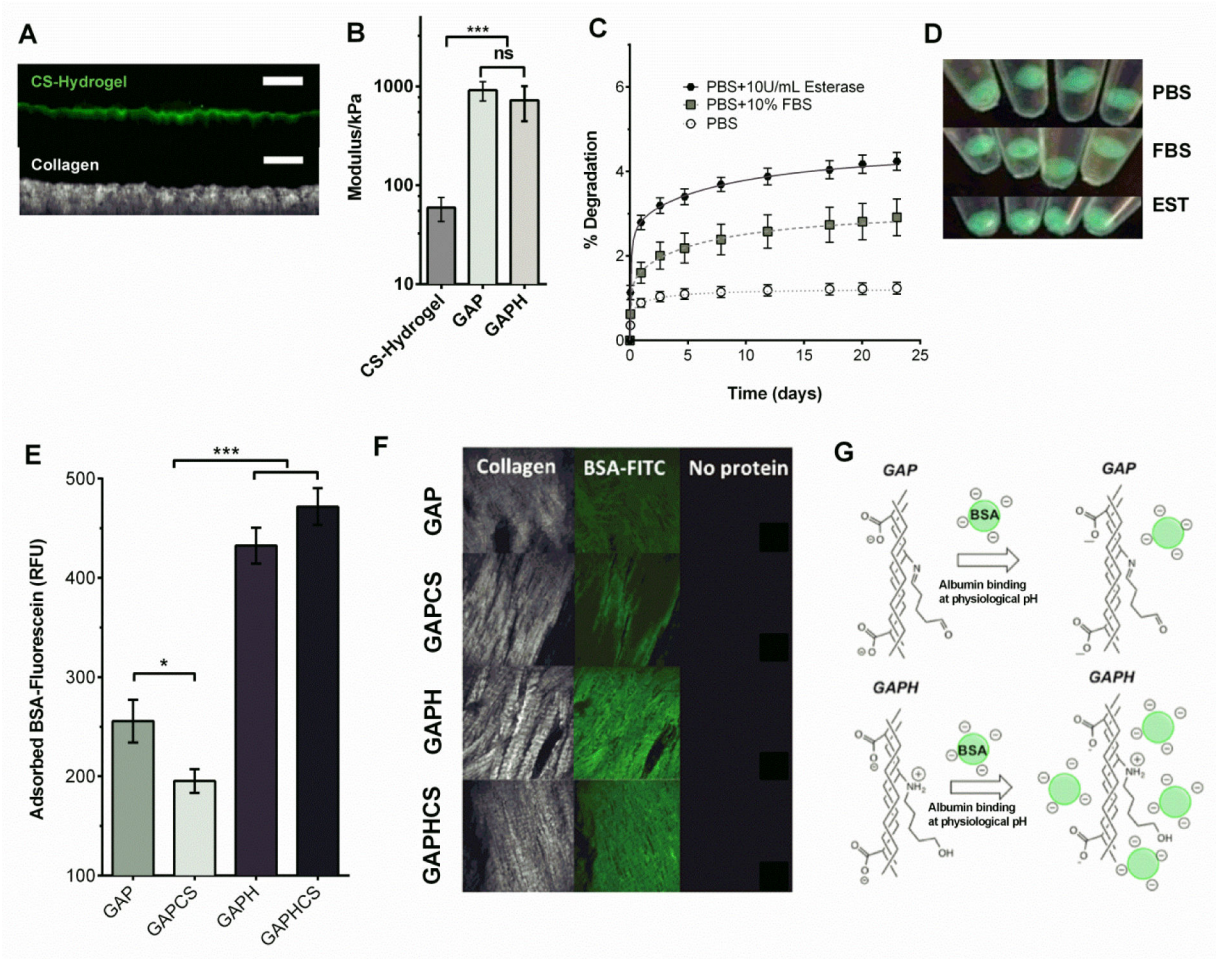

Figure 3. Hydrogel characterization and protein adhesion to tissues.

A, Chondroitin sulfate hydrogel (CS hydrogel) polymerized on the top of pericardium and cross-linked with fluorescein (green, top of the images), and collagen staining with the second harmonic generation obtained with multiphoton microscopy (white, bottom of the images), 50 μm scale bar. **B,** Modulus of the CS hydrogel and glutaraldehyde-fixed pericardium (GAP) or fixed and reduced pericardium (GAPH) patches. **C,** Degradation assay of the CS hydrogel cross-linked with fluorescein in phosphate buffer solution (PBS), PBS+ 10% fetal bovine serum (FBS), and PBS + esterase (EST). Quantification of fluorescein released to the solvent over time in relation to the initial cross-linked fluorescein in CS hydrogel. **D,** Integrity of CS hydrogels evaluated under UV-light after 20 days of incubation in PBS, PBS + 10% FBS and PBS with EST.. **E,** Quantification of fluorescein-labeled bovine serum albumin (BSA) adsorbed onto GAP, GAPH, GAP coated with CS hydrogel GAPCS, and GAPH coated with CS hydrogel (GAPHCS). **F,** Multiphoton imaging of collagen (left, white), adsorbed fluorescein-labeled bovine serum albumin (green, center) and background (Right) in GAP, GAPH, GAPCS, and GAPHCS. **G,** Scheme showing the interaction of albumin (negatively charged) with GAP and GAPH. GAP has no protonated groups at physiological pH and therefore a weak attraction for the negatively charged BSA. GAPH has secondary amines instead of imines and those are protonated at physiologic pH

suggesting a higher interaction with BSA and negatively charged proteins. Error bar ± SEM. Significant differences between the groups: * $p < 0.05$, *** $p < 0.001$.

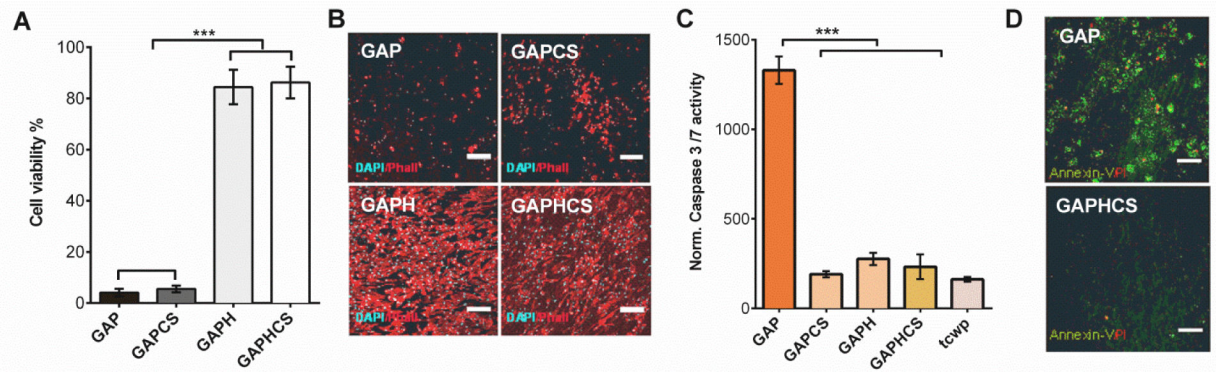

Figure 4. Endothelial cell viability and health in fixed pericardium after chemical reduction and addition of chondroitin sulfate hydrogel.

A, Cell viability of human aortic endothelial cells (HAEC) seeded for 3 days on top of fixed pericardium tissues. Cell viability is measured by quantifying the mitochondrial activity with the MTS assay. **B,** Staining of actin with phalloidin-TRITC (red) and DAPI (cyan) in HAEC seeded on glutaraldehyde-fixed pericardium (GAP) alone or with CS hydrogel (GAPCS), or on fixed and reduced pericardium (GAPH) alone or with CS hydrogel (GAPHCS) to analyze endothelial cell health; scale bar 200 μm. **C,** Activity of Caspase 3/7 normalized by the number of cells after 32 h. HAEC grown in tissue culture well-plates (tcwp) were used as control. **D,** Apoptosis in HAEC was further visualized with the phosphatidylserine exposure in the outer cell membrane stained by Annexin-V FITC conjugate (green). Propidium iodide (Red) was used to highlight necrosis in GAP and GAPHCS. Scale bar 75 μm. Histograms are plotted as mean ± SEM. Significant differences between the groups: *** $p < 0.001$.

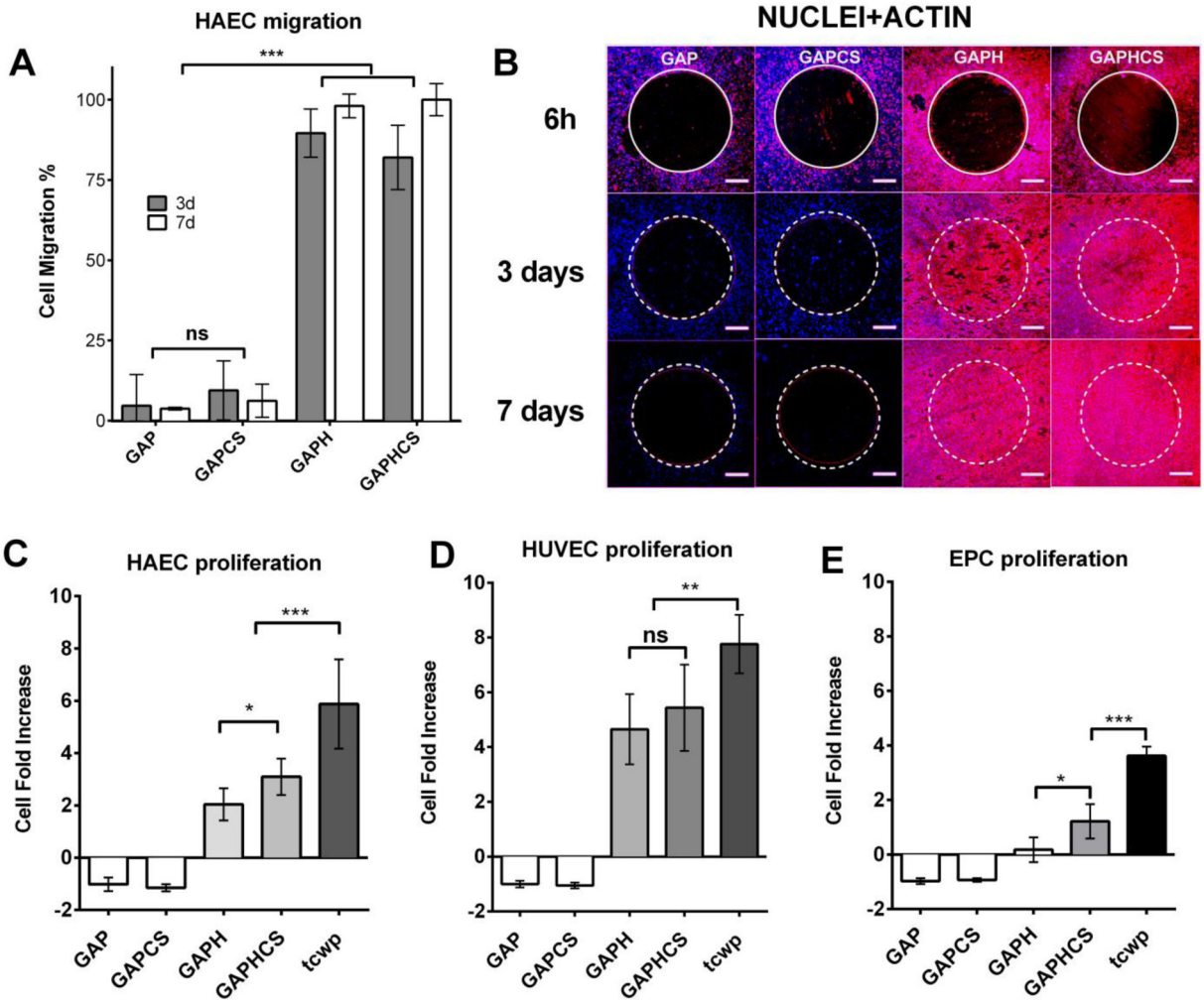

Figure 5. Migration and recruitment of endothelial cells and endothelial progenitor cells (EPC) after chemical reduction and addition of chondroitin sulfate hydrogel.

A, Quantification of the percentage of area invaded by the migration of human aortic endotheliai cells (HAEC) seeded around patches of glutaraldehyde-fixed pericardium (GAP) alone or with CS hydrogel (GAPCS), or on fixed and reduced pericardium (GAPH) alone or with CS hydrogel (GAPHCS) at different time points: 3 and 7 days. **B,** Staining of actin by phalloidin-TRITC (red) and DAPI (cyan) of the migrating cells. The original insert diameter is highlighted in yellow. 500 μm scale bar. Fold increase in proliferation after 7 days of incubation of HAEC **(C),** human umbilical vein endothelial cells (HUVEC) **(D)** and EPC **(E)** seeded on the top of pericardium-fixed tissues. Tissue culture well-plates (tcwp) of HAEC, EPC or HUVEC were used as controls. Histograms are plotted as mean ± SEM. Significant differences between the groups: * $p < 0.05$, ** $p < 0.01$, *** $p < 0.001$.

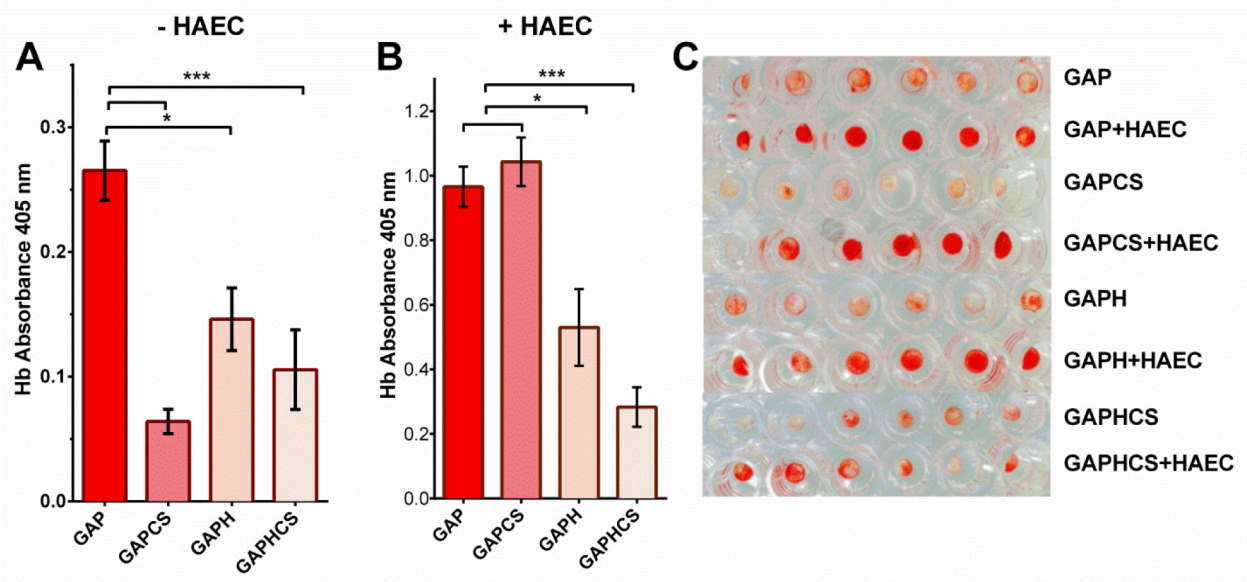

Figure 6. Blood clotting quantification of pericardium tissues after chemical reduction and addition of chondroitin sulfate hydrogel.

A, Direct incubation of pericardium patches with blood and quantification of the hemoglobin (Hb) absorvance at 405 nm to analyze the blood clotting of glutaraldehyde-fixed pericardium (GAP) alone or with CS hydrogel (GAPCS), or on fixed and reduced pericardium (GAPH) alone or with CS hydrogel (GAPHCS). **B,** Quantification of blood clotting in GAP, GAPCS, GAPH and GAPHCS after seeding human aortic endothelial cells (HAEC) on the top of the tissue leaflet. **C,** Imaging of blood clotting in GAP, GAPCS, GAPH and GAPHCS with or without HAEC. Histograms are plotted as mean ± SEM. Significant differences between the groups: * $p < 0.05$, *** $p < 0.001$.